Impact of the Methylene Bridge Substitution in Chelating NHC-Phosphine Mn(I) Catalyst for Ketone Hydrogenation

Ekaterina S Gulyaeva, Ruqaya Buhaibeh, Mohamed Boundor, Karim Azouzi, Jérémy Willot, Stéphanie Bastin, Carine Duhayon, Noël Lugan, Oleg A Filippov, Jean-baptiste Sortais, et al.

Chemistry–A European Journal
Research Article
doi.org/10.1002/chem.202304201
Chemistry Europe
European Chemical Societies Publishing
www.chemeurj.org

Impact of the Methylene Bridge Substitution in Chelating NHC-Phosphine Mn(I) Catalyst for Ketone Hydrogenation

Ekaterina S. Gulyaeva[+],[a, b] Ruqaya Buhaibeh[+],[a] Mohamed Boundor,[a] Karim Azouzi,[a] Jérémy Willot,[a] Stéphanie Bastin,[a] Carine Duhayon,[a] Noël Lugan,[a] Oleg A. Filippov,*[b] Jean-Baptiste Sortais,[a, c] Dmitry A. Valyaev,*[a] and Yves Canac*[a]

Systematic modification of the chelating NHC-phosphine ligand (NHC = *N*-heterocyclic carbene) in highly efficient ketone hydrogenation Mn(I) catalyst *fac*-[(Ph_2PCH_2NHC)$Mn(CO)_3Br$] has been performed and the catalytic activity of the resulting complexes was evaluated using acetophenone as a benchmark substrate. While the variation of phosphine and NHC moieties led to inferior results than for a parent system, the incorporation of a phenyl substituent into the ligand methylene bridge improved catalytic performance by *ca.* 3 times providing maximal TON values in the range of 15000–20000. Mechanistic investigation combining experimental and computational studies allowed to rationalize this beneficial effect as an enhanced stabilization of reaction intermediates including anionic hydride species *fac*-[($Ph_2PC(Ph)NHC$)$Mn(CO)_3H]^-$ playing a crucial role in the hydrogenation process. These results highlight the interest of such carbon bridge substitution strategy being rarely employed in the design of chemically non-innocent ligands.

Introduction

Metal-ligand cooperation[1] became nowadays a widespread tool for activation of inert chemical bonds by transition metal complexes often being relevant for homogeneous catalysis.[2] Pincer-type ligand systems (Scheme 1, top) originally introduced by Milstein[3] represents the emblematic example of such behavior exploiting facile de- and rearomatization of the central pyridine moiety *via* CH_2 bridge deprotonation and E–H bond activation steps, respectively. While the modification of this ubiquitous PNP architecture (Scheme 1, bottom) was mainly focused on variation of the donor side extremities[3–6] and more rarely of the central core,[7] the tuning of the methylene bridge yet directly involved in the cooperative event attracted much less attention. Indeed, only

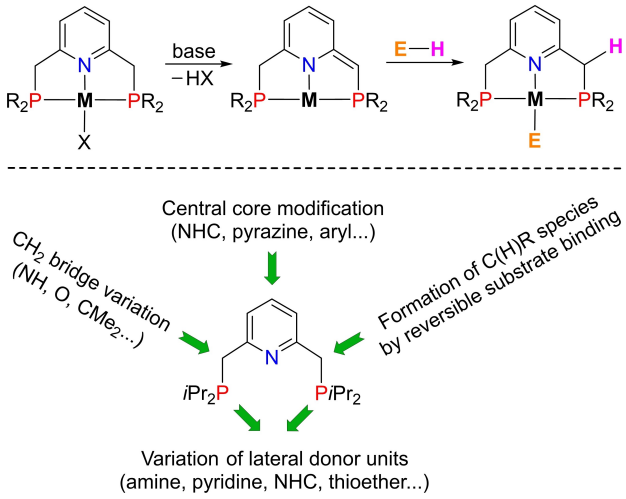

Scheme 1. Activation of inert bonds by metal-ligand cooperation *via* dearomatization of the central pyridine fragment in transition metal PNP pincer complexes (top) and structural modifications of this ligand scaffold (bottom).

the CH_2-to-NH replacement in such ligand scaffolds constitutes to date a major advance in this context,[8] whereas the incorporation of other fragments between the pyridine and the phosphine moieties such as "O"[9] and "CMe_2"[10] has been accomplished with the principal aim to inhibit the cooperative reactivity. Yet, reversible reactions of transition metal complexes bearing dearomatized phosphine-pyridine ligands with aldehydes,[11,12] ketones,[12] formates,[12] CO_2,[13] formamides,[14] isocyanates[14] and nitriles[15] was shown to give the products with bridge-substituted pincer scaffolds sometimes playing an important role in catalysis. Though numerous examples of bridge-modified pyridine-phosphine ligands[16] and their transition metal complexes[17,18] have

[a] *E. S. Gulyaeva,[+] Dr. R. Buhaibeh,[+] M. Boundor, Dr. K. Azouzi, Dr. J. Willot, Dr. S. Bastin, Dr. C. Duhayon, Dr. N. Lugan, Prof. Dr. J.-B. Sortais, Dr. D. A. Valyaev, Dr. Y. Canac*
LCC-CNRS, Université de Toulouse, CNRS, UPS
205 route de Narbonne, 31077 Toulouse Cedex 4, France
E-mail: dmitry.valyaev@lcc-toulouse.fr
yves.canac@lcc-toulouse.fr

[b] *E. S. Gulyaeva,[+] Dr. O. A. Filippov*
A. N. Nesmeyanov Institute of Organoelement Compounds (INEOS), Russian Academy of Sciences
28/1 Vavilov str., GSP-1, B-334, Moscow, 119334, Russia
E-mail: h-bond@ineos.ac.ru

[c] *Prof. Dr. J.-B. Sortais*
Institut Universitaire de France
1 rue Descartes, 75231 Paris Cedex 5, France

[+] *Both authors contributed equally to this work.*

Supporting information for this article is available on the WWW under https://doi.org/10.1002/chem.202304201

been reported in literature, the role of carbon-based substituent in the latter species was restricted to the modulation of steric properties,[17a–c] the incorporation of a chirality element[16c–d,17d] or as a spacer for covalent surface grafting.[17e,f] To the best of our knowledge, the direct influence of methylene bridge substitution on inert bond activation *via* metal-ligand cooperation was never investigated so far.

In this general context, we have recently reported the occurrence of dihydrogen activation *via* another type of metal-ligand cooperation in the NHC-phosphine Mn(I) complex *fac*-**2a** (NHC = *N*-heterocyclic carbene, unless necessary prefix *fac*- will not be further denoted for simplicity) involving the formation of unconventional NHC-phosphonium ylide species as a key step (Scheme 2, top).[19] This complex has proven to be a highly active catalyst for ketone hydrogenation with turnover numbers (TON) up to 6200. We report herein further tuning of this catalytic system in benchmark acetophenone hydrogenation through the diverse modifications of NHC-phosphine ligand (Scheme 2, bottom) and mechanistic studies related to the catalytic cycle.

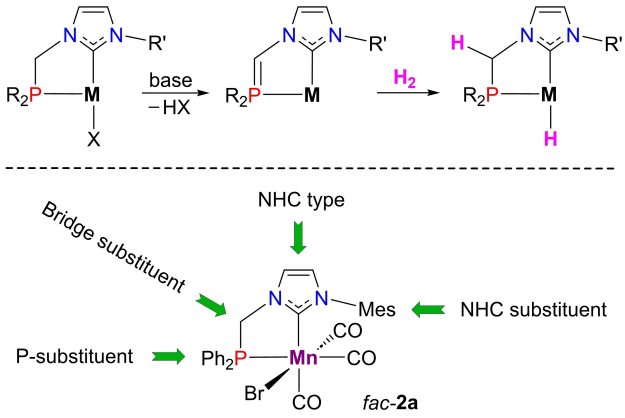

Scheme 2. General scheme of cooperative dihydrogen activation using chemical non-innocence of NHC-phosphine ligand (top) and structural variation of Mn(I) pre-catalyst for ketone hydrogenation performed in this work (bottom).

Results and Discussion

Synthesis and characterization of NHC-phosphine Mn(I) bromide complexes 2b–f

Phosphine-imidazolium pre-ligands [**1b–f**](OTs) (Scheme 3) have been prepared by four-step synthesis starting from readily available R_2PCl and azole derivatives (see the Supporting Information). The recently demonstrated beneficial effect of CH_2-to-C(H)Ph bridge substitution in the Mn(I) complex *fac*-[$(Ph_2PCH_2PPh_2)Mn(CO)_3Br$] for stoichiometric cooperative H_2 activation[20] and catalytic Guerbet reaction,[21] prompted us to consider a pre-ligand [**1e**](OTs) incorporating such C(H)Ph fragment. The latter may be accessible from Ph_2PH by a similar strategy in 20% overall yield or *via* previously published metal-mediated approach (BF_4^- salt, 3 steps starting from $CpMn(CO)_3$, 55% overall yield).[22] The deprotonation of the imidazolium salts [**1b–f**](OTs) with $KN(SiMe_3)_2$ (KHMDS) followed by complexation of the resulting free carbenes with [$Mn(CO)_5Br$] afforded the target Mn(I) complexes **2b–f** in good yield (Scheme 3).

All new Mn(I) complexes **2b–f** were fully characterized by IR and multi-nuclear NMR spectroscopy (see Table 1 for the most pertinent data). Solution IR spectra of complexes **2b–d** and **2f** in the ν_{CO} region display a typical three bands pattern characteristic for [(L–L')$Mn(CO)_3Br$] species with a facial arrangement of carbonyl groups. The analysis of ν_{CO} values does not show any clear trends besides the position of those with lowest frequencies, which seems to correlate with electronic properties of NHC-phosphine ligands reflecting in particular the stronger donation of iPr_2P *vs.* Ph_2P group. In contrast, for complex **2e** the splitting of the lowest frequency ν_{CO} band was observed, which was attributed to the existence of two isomers in solution differing by the position of hydrogen atom in the ligand bridge related to the bromide ligand similarly as it was found earlier for the related Mn(I) dppm complex *fac*-[$(Ph_2PCH(Ph)PPh_2)Mn(CO)_3Br$].[20] Two isomers were also detected by NMR spectroscopy in *ca.* 1:1.25 ratio (Table 1), showing in particular a downfield shift of the δ_P resonance by 10–20 ppm upon CH_2 bridge substitution. As in a parent complex **2a**, ^{13}C NMR spectra for **2b–f** revealed three distinct Mn–CO resonances with two types of $^2J_{CP}$ constants in a range of 16.7–21.3 Hz and 28.5–32.2 Hz, being

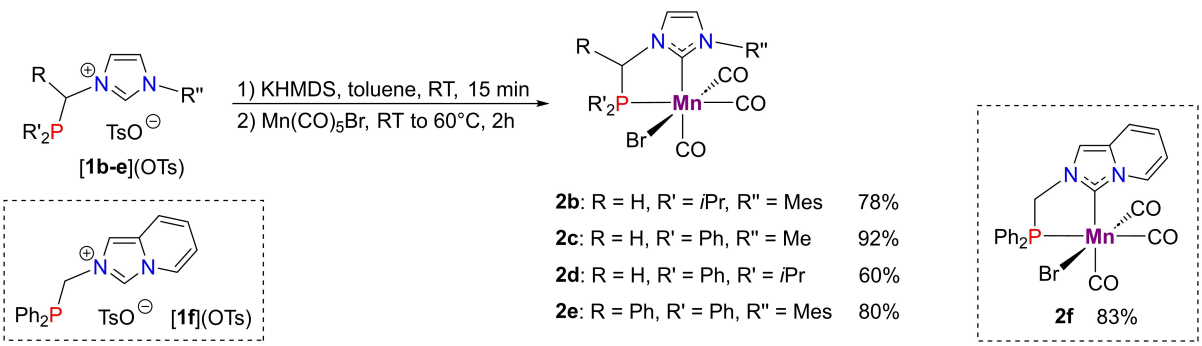

Scheme 3. Synthesis of Mn(I) complexes **2b–f** bearing bidentate NHC-phosphine ligands (inset contains the compounds derived from imidazo[1,5-*a*]pyridine).

Research Article
doi.org/10.1002/chem.202304201
Chemistry Europe
European Chemical Societies Publishing

Table 1. Selected IR[a] and NMR[b] data for bromide Mn(I) complexes **2a–f** bearing NHC-phosphine ligands.

N°	ν_{CO}	δ_P	δ_{NHC}	δ_{CO}
2a[c]	2017 vs, 1942 s, 1907 s	71.3	197.7	222.5, 219.8, 216.8
2b	2017 vs, 1944 s, 1892 s	91.0	197.9	225.1, 220.4, 217.2
2c	2014 vs, 1937 s, 1905 s	72.1	196.4	223.1, 221.3, 220.0
2d	2013 vs, 1935 s, 1905 s	70.6	194.9	223.6, 221.3, 220.3
2e[d]	2018 vs, 1948 s, 1906 m, 1896 m	93.8[a] 81.6[b]	198.9[b] 197.5[a]	225.0,[a] 222.5,[b] 219.6[a,b], 217.4,[a] 216.5[b]
2f[e]	2013 vs, 1939 s, 1903 s	72.2	187.7	222.6, 220,8, 219.2

[a] In THF solution, values are given in cm^{-1}. [b] In CD_2Cl_2 solution, values are given in ppm without $^2J_{CP}$ coupling constants for ^{13}C spectra (see the Supporting Information for details). [c] NMR data retrieved from ref. [19]. [d] Signals of major and minor isomer are indicated by [a] and [b], respectively. [e] NMR data in $CDCl_3$.

tentatively attributed to CO ligands situated in *cis*- and *trans*-position relative to the phosphine moiety, respectively. Carbene signals were typically found as doublets in a δ_C 194.9–198.9 ppm range with $^2J_{CP}$ coupling constants of 16.3–17.5 Hz with the exception of complex **2f**, for which a significant shielding was observed due to a different NHC skeleton. Molecular structures of complexes **2b–f** obtained by X-ray diffraction are shown in Figure 1.[23] All of them show a facial arrangement of three CO ligands, in a full agreement with spectral data in solution, represented in the case of complex **2e** by its *fac,syn*-isomer. Structural data within the five-membered metallacycles did not show any significant variation (Table S2) besides the P1–C4 bond in complex **2e** being *ca.* 0.04 Å longer compared to those in **2b–f** and in the parent analogue **2a**.[19]

Evaluation of NHC-Phosphine Mn(I) complexes 2b–e in catalytic hydrogenation of acetophenone

The catalytic activity of all Mn(I) NHC-phosphine complexes was evaluated in a benchmark hydrogenation of acetophe-

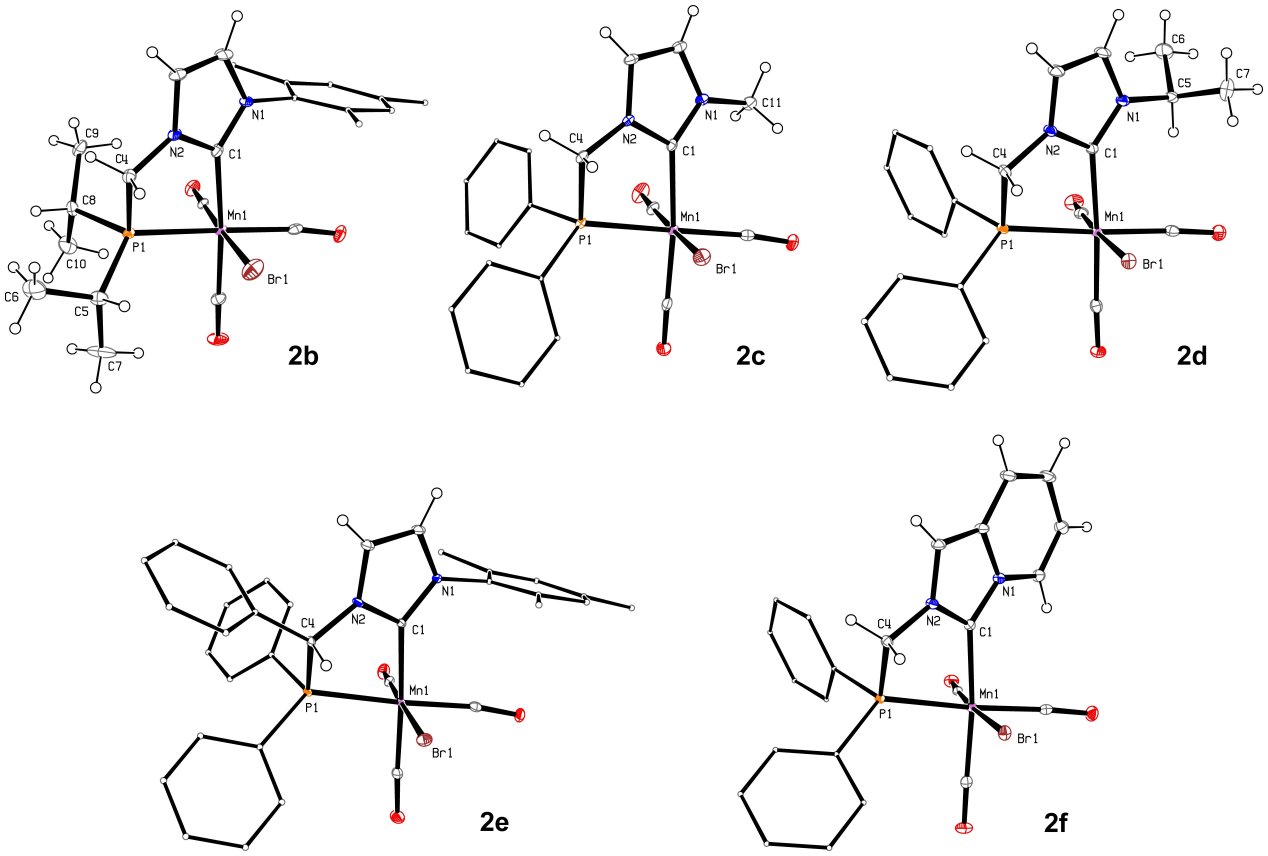

Figure 1. Molecular geometry of Mn(I) NHC-phosphine complexes **2b–e** (20% probability ellipsoids, aryl groups represented as a wireframe for clarity).

none (Table 2) using the experimental conditions previously optimized for complex **2a**.[19] Initial screening performed in toluene at 60 °C using 0.1 mol% of catalyst and 1.0 mol% KHMDS as a base (entries 1–5) revealed that only complex **2e** provided full substrate conversion, as it was observed for the CH_2 prototype **2a**.[19] While the variation of phosphine and NHC substituents globally kept excellent catalytic performance, the change of NHC scaffold (entry 5) clearly led to poorer results. The four most efficient Mn(I) complexes **2b–e** were then tested at the same catalyst loading in *t*AmOH at 60 °C using 1.0 mol% of *t*BuOK as a base (entries 6–9) providing an improvement of the catalytic performance for **2b** and **2d**. Further decrease of the catalyst charge to 0.05 mol% (entries 10–13) allowed us to identify the two best systems based on **2b** and **2e** and thus highlighted the importance of steric hindrance of the NHC substituent (Mes > *i*Pr > Me) in this process. The comparison of two best catalysts **2b** and **2e** at 0.01 mol% loading (entries 14–15) showed that the latter was ca. 1.5 times more productive. In order to approach the limits of this system we have carried out two sets of experiments using 50 and 10 ppm catalyst charge at 60 and 100 °C (entries 16–19) to give TONs in a 15000–20000 range surpassing significantly the results achieved with original catalyst **2a** (TON 6200 at 100 °C).[19]

Table 2. Acetophenone hydrogenation catalyzed by Mn(I) NHC-phosphine complexes **2b–f**.[a]

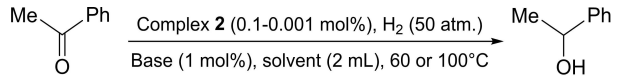

N°	[Cat] (mol%)	Base	Solvent	T, °C	Conv. %[b]	TON[b]
1	**2b** (0.1)	KHMDS	Toluene	60	82	820
2	**2c** (0.1)	KHMDS	Toluene	60	74	740
3	**2d** (0.1)	KHMDS	Toluene	60	62	620
4	**2e** (0.1)	KHMDS	Toluene	60	>99	1000
5	**2f** (0.1)	KHMDS	Toluene	60	0[c]	–
6	**2b** (0.1)	*t*BuOK	*t*AmOH	60	>99	1000
7	**2c** (0.1)	*t*BuOK	*t*AmOH	60	73	730
8	**2d** (0.1)	*t*BuOK	*t*AmOH	60	94	940
9	**2e** (0.1)	*t*BuOK	*t*AmOH	60	>99	1000
10	**2b** (0.05)	*t*BuOK	*t*AmOH	60	>99	2000
11	**2c** (0.05)	*t*BuOK	*t*AmOH	60	22	440
12	**2d** (0.05)	*t*BuOK	*t*AmOH	60	64	1280
13	**2e** (0.05)	*t*BuOK	*t*AmOH	60	>99	2000
14	**2b** (0.01)	*t*BuOK	*t*AmOH	60	57	5700
15	**2e** (0.01)	*t*BuOK	*t*AmOH	60	88	8800
16	**2e** (0.005)	*t*BuOK	*t*AmOH	60	43	8600
17	**2e** (0.001)	*t*BuOK	*t*AmOH	60	16	16000
18	**2e** (0.005)	*t*BuOK	*t*AmOH	100	76	15200
19	**2e** (0.001)	*t*BuOK	*t*AmOH	100	21	21000

[a] Typical procedure: an autoclave was charged with Mn(I) pre-catalyst, ketone (2.0 mmol), base (1.0 mol%), solvent (2 mL) in this order and then rapidly pressurized with H_2 (50 bar) and heated under stirring for 20 h at the indicated temperature. [b] Conversion and TON were determined by the analysis of crude product by ^{1}H NMR spectroscopy (average value of two independent runs). [c] 97% conversion was obtained using 1.0 mol% of catalyst.

Despite remarkable progress in Mn-catalyzed hydrogenation reactions,[24] the typical catalyst loading for ketone hydrogenation still remains in a range of 0.5–2.0 mol%[25,26] rarely decreasing for some substrates to 0.1 mol%[25i,m] or even below.[25f–i] The catalytic performance of complex **2e** is comparable with those obtained using Mn(I) PNN pincer complexes (TONs 9800–13000)[25f–h] and inferior only to the extremely active Mn(I) complex based on NHC-amine-phosphine pincer ligand providing up to 200000 TONs for the hydrogenation of acetophenone at 100 °C.[27] The results obtained in this work as well as recent literature data[7a,25a,27,28] illustrate once more the great potential of NHC-based ligands in the design of highly efficient and robust Mn-based catalysts for (de)hydrogenation-type processes.

Experimental and theoretical investigations of the cooperative dihydrogen activation by NHC-phosphine Mn(I) complex 2e

In order to rationalize the better catalytic efficiency of complex **2e** exhibiting a C(H)Ph ligand bridge, we first decided to study stoichiometric H_2 activation relevant to pre-catalyst activation step. The treatment of **2e** with KHMDS in toluene at room temperature rapidly led to the formation of NHC-phosphinomethanide complex **3e** (Scheme 4) being virtually quantitative according to IR spectroscopy data (Figure 2). In contrast to its parent analogue **2a** requiring a considerable excess of KHMDS (2.5 equivalents) to achieve full **2a**→**3a** conversion,[19] the deprotonation of **2e** under the same conditions is much easier probably due to the increase of C–H bond acidity by the presence of phenyl substituent. Notably, complex **3e** shows no signs of decomposition in C_6D_6 solution after several hours at room temperature being much more thermally stable than its analogue **3a** decomposing even at −30 °C in [D_8]toluene.[19]

The chemical identity of cyclometallated complex **3e** was elucidated from IR and NMR spectroscopy data. Solution IR spectrum (Figure 2) contains three ν_{CO} bands at 1992 s, 1908 sh and 1900 s being in agreement with a facial arrangement of three CO ligands. ^{31}P NMR spectrum of **3e** exhibited a sole resonance at δ_P 60.9 ppm indicating the transformation

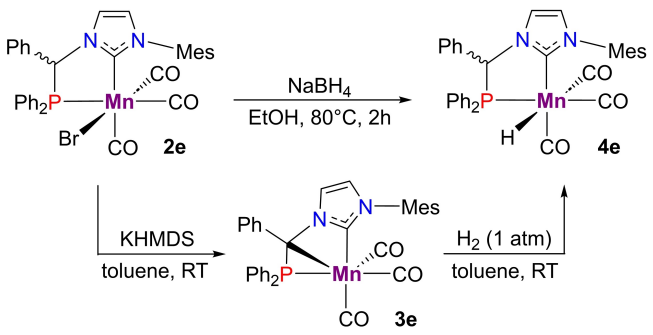

Scheme 4. Cooperative dihydrogen activation by NHC-phosphinomethanide complex **3e** generated by deprotonation of Mn(I) NHC-phosphine precursor **2e**.

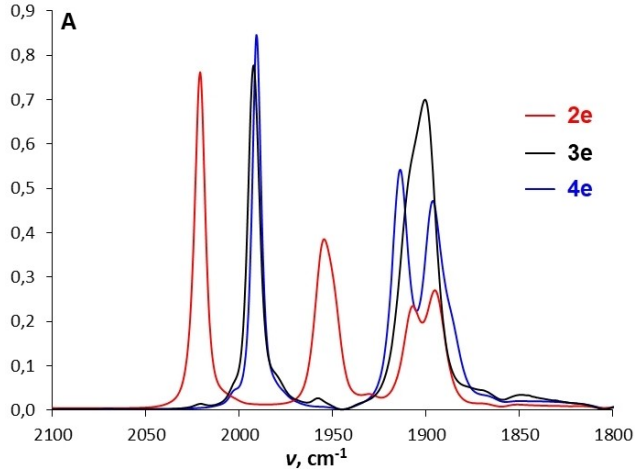

Figure 2. IR spectroscopy monitoring of the deprotonation of complex **2e** and subsequent reaction of the cyclometallated species **3e** with dihydrogen (2100-1800 cm^{-1} region, toluene, 0.1 mm CaF_2 cell).

of both isomers of **2e** into a single compound. The ^{13}C resonance of the coordinated bridging carbon atom in **3e** was observed as a doublet at δ_C 40.7 ppm ($^1J_{PC}$ = 19.5 Hz) deshielded compared to those in **3a** (δ_C 22.7 ppm)[19] or related κ^3-PCN (δ_C 9.6–10.1 ppm) and κ^3-PCP (δ_C −10.1–−12.8 ppm) cyclometallated Mn(I) species derived from phosphine-pyridine[29] and dppm-type[20] scaffolds, respectively. Finally, the signals of coordinated NHC and carbonyl ligands in **3e** were observed as a doublet at δ_C 180.0 ppm ($^2J_{PC}$ = 16.8 Hz) and two broad resonances at δ_C 227.5 and 223.6 ppm, similar to those of compound **3a**.[19]

Hydrogen bubbling through the toluene solution of **3e** at room temperature led to rapid and spectroscopically quantitative (Figure 2) formation of the hydride complex **4e** (Scheme 4) isolated in 80% yield. The same product as well as its CH_2 analogue **4a** can be also prepared directly from the corresponding bromide precursors by a thermal reaction with an excess of $NaBH_4$ in ethanol (Scheme 4) using a protocol previously established for Mn(I) complexes bearing diphosphine[30] and bis(NHC)[31] ligands.

According to multi-nuclear NMR spectroscopy data hydride complex **4e** exists in C_6D_6 solution as a mixture of two isomers in *ca.* 4:1 ratio, the major one being assigned to *fac,anti*-**4e** from 1D NOE NMR experiments (see the Supporting information). In contrast to its bromide precursor **2e** (Table 1, Figure 2), both isomers of **4e** have nearly identical IR spectra characteristic of typical facial carbonyl ligand arrangement. Hydride signals for *fac,anti*-**4e** and *fac,syn*-**4e** were observed as doublets at δ_H −6.49 ($^2J_{PH}$ = 52.3 Hz) and −6.73 ($^2J_{PH}$ = 51.7 Hz) ppm respectively, exhibiting in both cases coupling constant values characteristic for a *cis*-arrangement of hydride and phosphine fragments. The position of NHC signal in ^{13}C NMR of the major isomer of **4e** (δ_C 205.9 ppm, $^2J_{PC}$ = 16.5 Hz) was shifted downfield by *ca.* 10 and 25 ppm related to those of **2e** and **3e**, respectively.

To gain more insights, the interaction of complex **3e** with dihydrogen was calculated at BP86/def2-TZVP level in toluene at 298 K (see the Supporting Information for details). Analysis of the superposed ΔG^{298} profiles for **3a**[19] and **3e** (Scheme 5) shows lower energy span for the overall **3e**→ *fac,syn*-**4e** transformation thus indicating easier cooperative H_2 activation for phenyl-substituted derivative. The most notable difference between these two cooperative systems concerns the activation barriers for the formation of non-classical NHC-ylide intermediates **5** and their relative stability *vs.* initial NHC-phosphinomethanide complexes **3**. The two-fold decrease of the energy for transition state **TS1e** may be rationalized by weaker Mn–C(R) bond in **3e**, which was reflected both by longer distance (**3e**: 2.268 Å; **3a**: 2.186 Å) and smaller Wiberg bond index (WBI)[32] (**3e**: 0.318; **3a**: 0.370). Lower ring strain in **3e** was also evidenced by smaller value of yaw angle θ[33] for the NHC coordination (28.5°) *vs.* that in **3a** (29.5°)[19] being consistent with the position of respective ^{13}C carbene resonances.[34] This situation differs from the reactivity of related Mn(I) complexes bearing dppm ligands,[20] in which easier cooperative H_2 activation in bridge-substituted derivatives was mainly attributed to higher steric destabilization of bicyclic MnPCP system. Calculated P=C bond lengths in **5** and **6** (1.717–1.734 Å) are comparable with those experimentally observed for Mn(I) (1.73(1) Å)[35] or Fe(II) (1.766(11) Å)[36] derivatives bearing non-classical ylide ligands and Pd(II) complexes with conventional NHC-ylide ligands (1.750(7)–1.794(8) Å).[37] Despite the ligand bridge modification in complexes **5** and **6** does not significantly influence structural data (Table S3), Ph-substituted derivatives are more stable than their CH analogues. This effect was rationalized in terms of higher delocalization of the negative charge at the ylidic carbon atom in **5e** (−0.306) and **6e** (−0.435) *vs.* **5a** (−0.527) and **6a** (−0.730), actually being reminiscent of the well-known situation found in the chemistry of non-stabilized and semi-stabilized free phosphonium ylides.[38]

According to DFT calculations the transformation of *fac,syn*-**4e** into its more stable *fac,anti*-**4e** isomer (Scheme 6) proceeds *via* a sequential synchronous rotation of the entire [$Mn(CO)_3H$] moiety with the intermediate formation of less stable meridional hydride intermediate *mer*-(*P*)-**4e** (see Supporting Information for details). The activation barriers values for **TS4** and **TS5** are very close to those previously calculated for the isomerization of *fac,syn*-[($dppm^{Ph}$)$Mn(CO)_3H$][20] being in agreement with the occurrence of this dynamic process at room temperature. These results also allowed us to understand the intriguing formation of an equimolar mixture of hydride products upon the reaction of complex **3a** with D_2 gas.[19]

Insights into the catalytic cycle of ketone hydrogenation catalyzed by NHC-phosphine Mn(I) complexes 2a and 2e

We have next performed the DFT modelling of the catalytic cycle for acetophenone hydrogenation from manganese hydrides **4a** and **4e**. First, we examined the possibility of an inner-sphere hydride transfer mechanism previously evi-

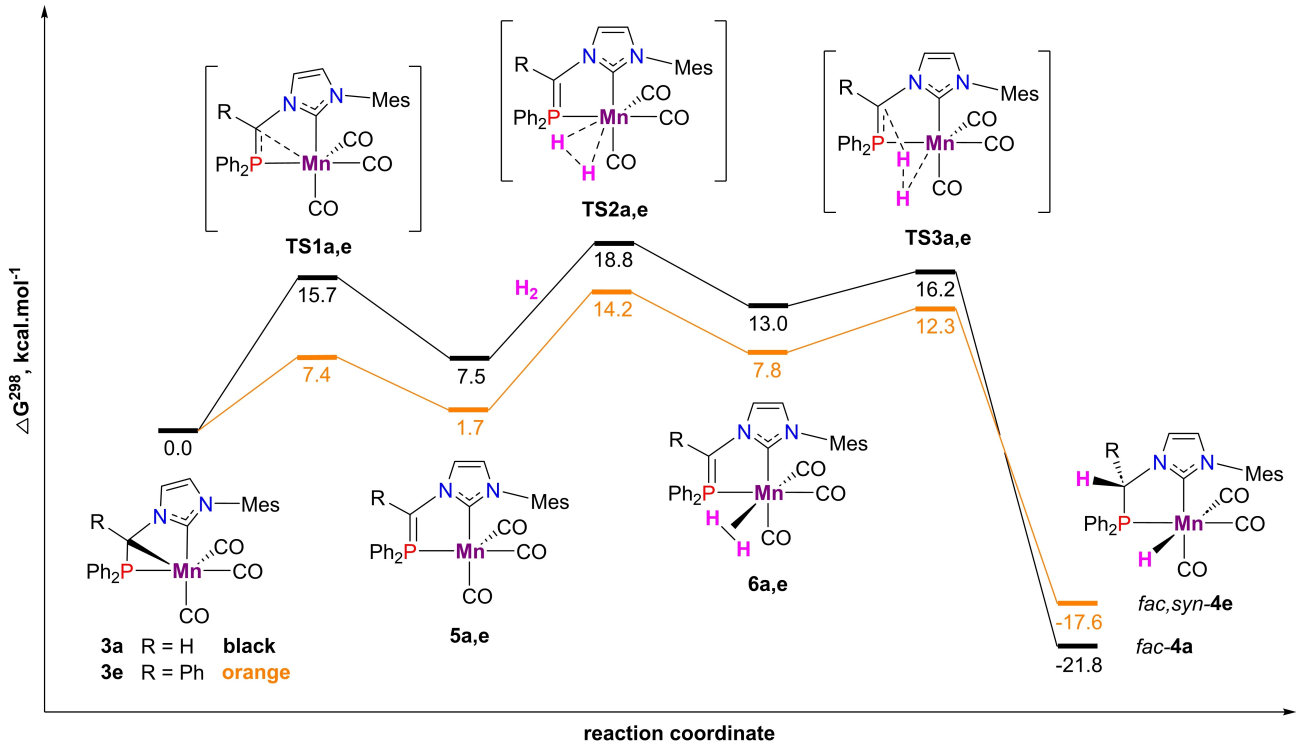

Scheme 5. The comparison of Gibbs energy profiles for cooperative dihydrogen activation with Mn(I) NHC-phosphinomethanide complexes **3a** (R = H)[19] and **3e** (R = Ph) at BP86/def2TZVP calculation level using toluene as SMD model (values are given in kcal.mol^{-1} and referred to **3a** or **3e** for each profile). Transition state **TS2e** was localized using slightly simplified model with a phenyl substituent at the NHC moiety.

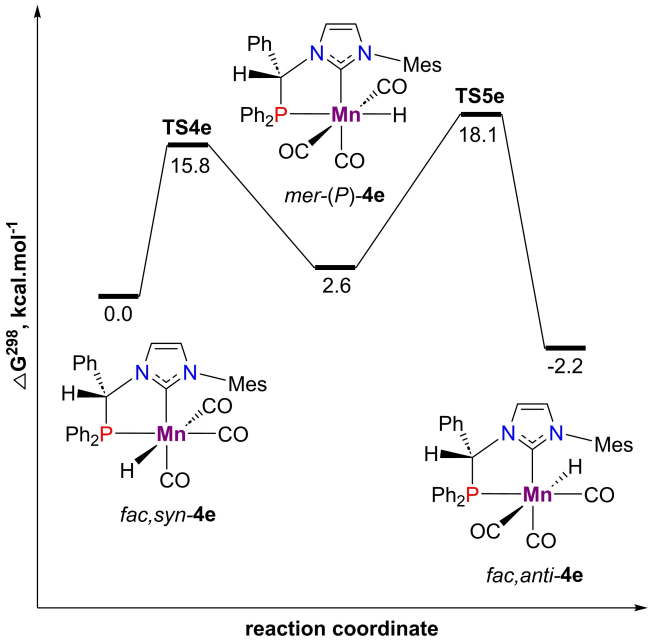

Scheme 6. Gibbs energy profile for the isomerization of Mn(I) hydride complex *fac,syn*-**4e** (BP86/def2-TZVP calculation level using toluene as SMD model).

denced in ketone hydrogenation using Mn(I) PNP[25j] and NN[26a] complexes. However, we were unable to locate transition states between hydride complexes **4a,e** and acetophenone leading to the formation of the corresponding alkoxide species *fac*-[$(Ph_2PCH(R)NHC)(CO)_3MnOCH(Me)Ph$]. Considering a previous theoretical investigation on CO_2-to-MeOH hydrogenation using complex **4a** and its $(iPr)_2P$ analogue,[39] we then checked the possibility of the existence of a concerted Noyori-type mechanism[40] with the direct participation of non-innocent NHC-phosphine ligand as proton donor. The superposition of Gibbs energy profiles for the interaction of Mn(I) hydride complexes **4a** and *fac,syn*-**4e** with acetophenone obtained at ωB97XD/def2TZVP level using *t*BuOH as a solvent (SMD model) is shown in Scheme 7. The reaction for both hydrides starts with the formation of van der Waals adducts **4**···Me(Ph)C=O destabilized by 6.0 and 4.7 kcal.mol^{-1} relative to the initial mixture of **4a** and **4e** with acetophenone, respectively. These intermediates transform *via* concerted transition states **TS6** into the corresponding NHC-ylide complexes with non-covalently bound alcohol **5**···Me(Ph)CHOH, which then undergo the dissociation and regeneration of the starting hydrides **4** in a presence of dihydrogen (*vide supra*). However, calculated activation barriers for **4**···Me(Ph)C=O→**5**···Me(Ph)CHOH transformation (*ca.* 28 kcal.mol^{-1}) seem to be quite elevated for the catalytic process rapidly proceeding at 60 °C and such concerted hydride/proton transfer mechanism is in discrepancy with experimental data. Despite complex **4a** can be successfully used as pre-catalyst,[19] no catalytic activity was observed using up to 5 mol % of isolated Mn(I) hydride species **4a** and **4e** in the absence of base at 60 °C in toluene or *t*AmOH. In

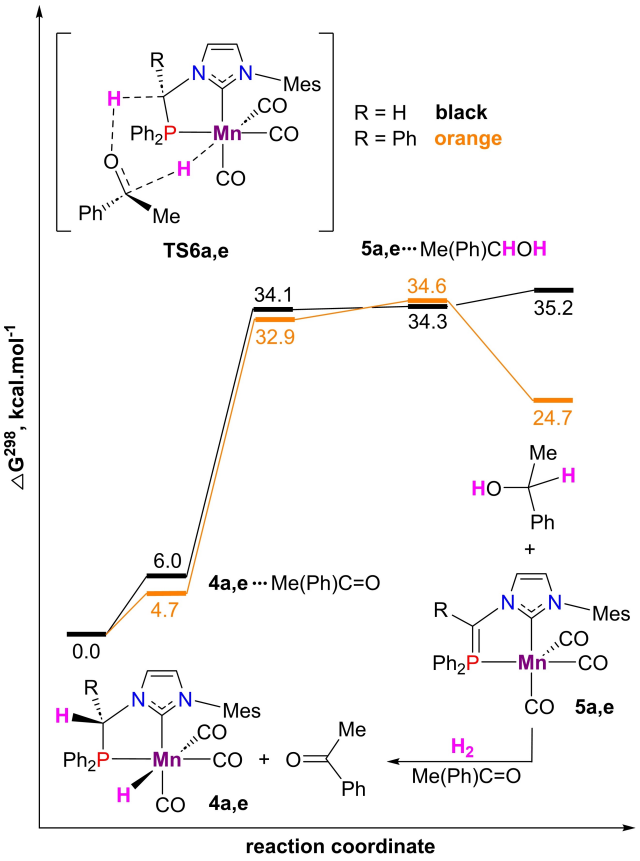

Scheme 7. Gibbs energy profiles for the concerted reaction of Mn(I) hydride complexes **4a** (black) and *fac,syn*-**4e** (orange) with acetophenone (ωB97XD/def2TZVP calculation level using *t*BuOH as SMD model). The formation of non-covalent adducts between Mn(I) complexes and organic molecules is indicated by dotted bonds.

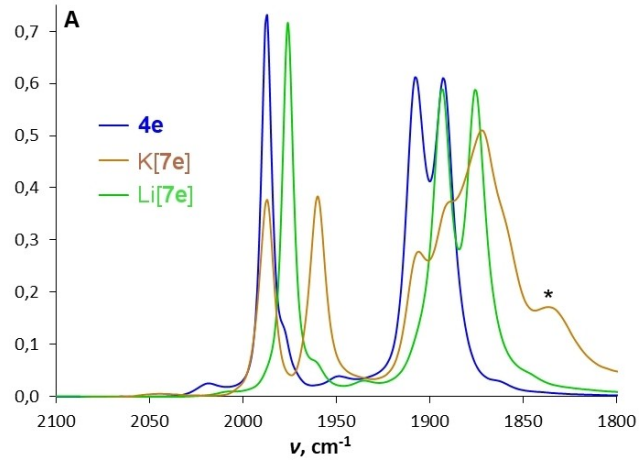

Figure 3. IR spectroscopy monitoring of the deprotonation of hydride complex **4e** with 5 equivalents of KHMDS or LDA (2100-1800 cm^{-1} region, THF, 0.1 mm CaF_2 cell). The peak belonging to an unidentified decomposition product of complex K[**7e**] is marked with asterisk.

addition, these hydride complexes were found completely intact upon heating at 60 °C with an excess of ketones (acetophenone, benzophenone) in various solvents (toluene, THF, *t*AmOH) thus indicating that the real mechanistic pattern is *a priori* more complicated.

Inspired by our recent observation of backbone C–H bond deprotonation in complex *fac*-[(dppm)Mn(CO)$_3$H][41] as well as growing literature evidence for the implication of anionic Mn(I) and Ru(II) hydrides supporting by PNP,[42] PNN,[43,44] PCP[7a] and NN[26a,45] ligands in catalytic hydrogenation-type processes, we investigated reactivity of Mn(I) NHC-phosphine hydride complexes **4** with strong bases. It was shown that the treatment of **4e** with a large excess of KHMDS (5 eq.) in THF at −30 °C led to its partial conversion to a novel thermally unstable species K[**7e**] featuring two main ν_{CO} bands at 1960 and 1872 cm^{-1} (Figure 3). ^{31}P NMR analysis of the sample generated in [D$_8$]THF at −30 °C revealed a new signal at δ_P 79.3 ppm, significantly shielded compared to those of *fac,syn*-**4e** and *fac,anti*-**4e** observed at δ_P 112.7 and 117.5 ppm, respectively. The relatively small low frequency shift of ν_{CO} bands in K[**7e**] being inconsistent with the formation of anionic carbonylate complex as well as the detection of hydride resonance at δ_H −6.87 ppm (d, $^2J_{PH}$ = 45.3 Hz) allow us to propose that the deprotonation event takes place at the C(H)Ph bridge of NHC-phosphine ligand. The attempted deprotonation of *a priori* less acidic complex **4a** with KHMDS under the same conditions led to a complicated mixture of products according to IR and ^{31}P NMR data probably due to extensive decomposition of the resulting product. Similar trend was recently observed in the deprotonation of Pd(II) complexes bearing CH_2- and C(H)Ph-bridged NHC-phosphine fragments.[46]

Gratifyingly, the use of a stronger base such as LiN*i*Pr$_2$ (LDA) for the deprotonation of **4e** led to a quasi-quantitative formation of the anionic complex Li[**7e**] (Figure 3). While the key ^{1}H and ^{31}P NMR characteristics were found to be similar for those of K[**7e**], the IR spectrum of Li[**7e**] is quite different showing *ca.* 15 cm^{-1} high frequency shift of ν_{CO} bands. Vibrational analysis of possible optimized structures for complex [**7e**]$^-$ containing both alkali metals showed very good agreement with experimental data and revealed that in the most stable isomer of Li[**7e**] lithium cation is tightly bound to the bridging carbon atom, whereas its potassium analogue is highly dissociated in THF solution and exists as solvent-separated ion pair (see Supporting Information for details). Complex Li[**7e**] was fully characterized by multi-nuclear NMR spectroscopy at −30 °C revealing in particular a quaternary carbon signal at δ_C 71.8 ppm ($^1J_{PC}$ = 88.5 Hz), which clearly confirms the deprotonation of the C(H)Ph bridge.

In contrast to the inertness of neutral hydride **4e** towards ketones, the addition of benzophenone (2 equiv.) to THF solutions of K[**7e**] or Li[**7e**] at −30 °C followed by warming to room temperature and hydrolysis allowed to detect by NMR the formation of the corresponding alcohol Ph_2CHOH (see the Supporting information). The same product was also identified in the mixture of complex **4a**/KHMDS/Ph_2C=O being in agreement with a transient formation of the anionic intermediate K[**7a**]. Similar reactivity trend between neutral and anionic Mn(I) hydrides with styrene was very recently observed by Kirchner et al. in complexes bearing P-NHC–P ligands.[7a] These results

Table 3. Selected bond distances, NBO charges and Hydride Donating Abilities (HDA, in kcal.mol^{-1}) for neutral and anionic Mn(I) NHC-phosphine hydride complexes calculated at ωB97XD/def2TZVP level using *t*BuOH as SMD model.

Complex	Bond lengths, Å		Selected NBO6 charges			HDA,
	P–C_{br}	Mn–H	H_{Mn}	C_{br}	$Mn(CO)_3$	ΔG^{298}
4a	1.843	1.595	−0.104	−0.531	−0.708	45.4
fac,anti-**4e**	1.881	1.605	−0.113	−0.335	−0.687	48.9
[**7a**]$^-$	1.739	1.604	−0.137	−0.849	−0.768	35.2
[**7e**]$^-$	1.750	1.605	−0.143	−0.504	−0.733	35.5
fac,anti-Li[**7a**]	1.780	1.596	−0.122	−0.929	−0.767	42.7
fac,Ph-Li[**7e**]	1.762	1.594	−0.125	−0.478	−0.711	39.0

are perfectly in line with well-known superior hydricity of anionic transition metal complexes *vs.* their neutral congeners estimated either experimentally[42a,d,47] or by theoretical means.[42a–b,45]

The examination of molecular geometry in calculated **4a**/[**7a**]$^-$ and *fac,anti*-**4e**/[**7e**]$^-$ couples (Table 3) shows a shortening of the P–C(R) bond by *ca.* 0.1 Å upon NHC-phosphine bridge deprotonation, whereas Mn–H bond remains almost unaffected. As expected, the charges at the bridging carbon atom (C_{br}) in [**7a**]$^-$ and [**7e**]$^-$ become much more negative compared to those in the corresponding neutral species contrasting with smaller charge variation at the hydride ligand and $[Mn(CO)_3]$ moiety. These results together with experimental IR spectroscopy data (*vide supra*) indicate that the electronic structure of hydride complexes [**7a**,**e**]$^-$ (Scheme 8) is closer to the resonance form **A** exhibiting anionic phosphine-NHC scaffold rather than to the manganate species **B** featuring non-classical NHC-ylide ligand.

Taking into account different reactivity of neutral and anionic Mn(I) hydrides with ketones, we have quantified their Hydride Donating Ability (HDA) defined as the calculated Gibbs energy of $[M]^n–H \rightarrow [M]^{n+1} + H^-$ transformation (Table 3). While in the neutral hydride series **4a** was found to be more hydridic than **4e** (ΔHDA 3.5 kcal.mol^{-1}), the difference of hydricity becomes negligible for anionic complexes [**7a**,**e**]$^-$ showing unexpectedly significant increase of HDA value upon deprotonation of the C(H)Ph bridge. Being aware of potential bias related to the direct comparison of HDA values for differently charged systems,[48] we have carried out similar investigation taking into account counter-cation effect using Li^+ as a simplest relevant model (see Supporting Information for details). Gratifyingly, it was shown that structurally close *fac,Ph*-isomer of complex Li[**7e**] was again more hydridic than its non-substituted analogue Li[**7a**] (Table 3), which was also in agreement with slightly higher negative charges at the hydride ligands evidenced in both free [**7a**]$^-$/[**7e**]$^-$ and cation stabilized Li[**7a**]/Li[**7e**] pairs.

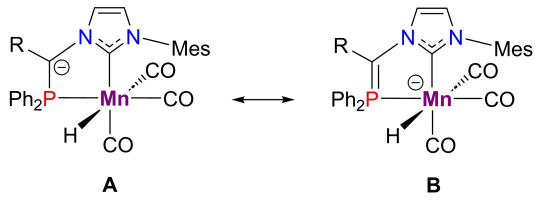

Scheme 8. Two resonance forms describing the electronic structure of anionic Mn(I) hydride complexes [**7a**]$^-$ (R = H) and [**7e**]$^-$ (R = Ph).

Finally, we have calculated the Gibbs energy profile of the interaction of anionic Mn(I) hydrides with acetophenone using *t*BuOH as a solvent (SMD model) (Scheme 9). Unlike the previous concerted mechanism (Scheme 7), it was shown that the presence of *t*BuOH molecule is crucial for the stabilization of key stationary points at potential energy surface, whereas the well-documented assistance of potassium cation in hydride transfer[40] was not evidenced in our case. The reaction begins with a formation of van der Waals adducts [**7**]$^-$···Me-(Ph)C=O···HO*t*Bu, which then undergo a direct outer-sphere hydride transfer[49] to ketone *via* **TS7** leading to NHC-ylide complexes **5** associated with $Me(Ph)CHO^-$ anion hydrogen bonded to *t*BuOH molecule. The subsequent dissociation of the latter ternary intermediate followed by cooperative H_2 activation by complexes **5** and the deprotonation of the resulting hydrides **4** closes the catalytic cycle. The highest activation barriers found in this case are 8–10 kcal.mol^{-1} lower than for the concerted proton/hydride transfer mechanism (Scheme 7) being largely accessible under experimentally used temperature for catalytic hydrogenation (60–100 °C).[50] Similar trend for inner-sphere hydride transfer from neutral and anionic Mn(I) NN-complexes to acetophenone with calculated activation Gibbs energies of 27.7 and 19.4 kcal.mol^{-1}, respectively was very recently found by Mösch-Zanetti and coll.[26a] Interestingly, in contrast to cooperative H_2 activation step (Scheme 5) the energy span for Ph-substituted complex [**7e**]$^-$ was calculated to be slightly higher than for [**7a**]$^-$. We can therefore conclude that superior catalytic performance of complex **2e** is likely caused by a better stability of the different key species in this catalytic cycle namely the unsaturated NHC-ylide complex **5e**, its cyclometallated isomer **3e** and anionic hydride derivative K[**7e**].

Conclusions

We have performed various structural modifications of highly active system for ketone hydrogenation based on NHC-phosphine Mn(I) complex **2a** and investigated in details using

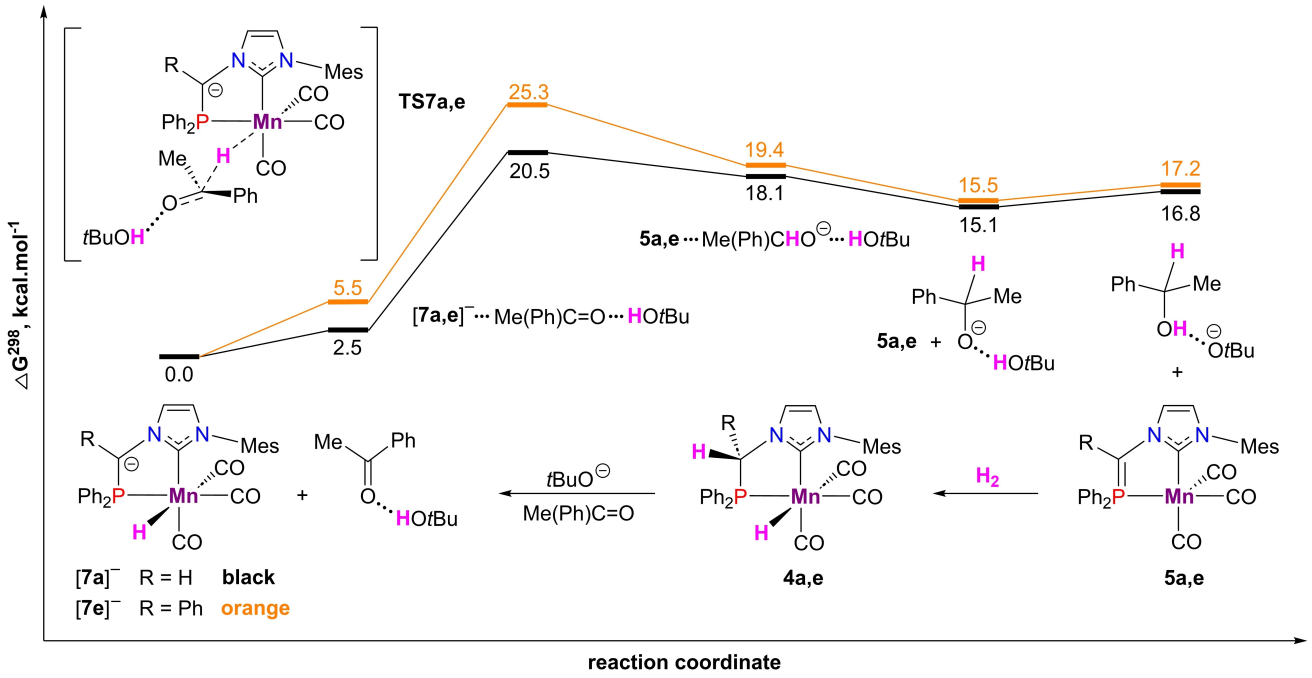

Scheme 9. Gibbs energy profiles for the reaction between Mn(I) hydride complexes [**7a**]$^-$ (black) and [**7e**]$^-$ (orange) and acetophenone with the assistance of *t*BuOH molecule (ωB97XD/def2TZVP calculation level using *t*BuOH as SMD model). Non-covalent interactions are indicated by dotted bonds.

spectroscopic and computational tools the nature of metal intermediates and overall mechanism of this catalytic process. Importantly, the incorporation of a phenyl substituent to the bidentate ligand methylene bridge allowed to boost the performance of the parent catalyst providing impressive TON values for hydrogenation of acetophenone. This unexpected effect was perfectly rationalized as a combination of easier activation of the initial Mn(I) bromide pre-catalyst due to increased C–H bond acidity and stability of the main intermediates of the catalytic cycle including in particular anionic Mn(I) hydride complex essential for hydride-ion transfer to ketone substrate. We assume that the extension of this aryl-substitution concept to other known cooperative systems based on methylene bridge deprotonation may be of potential interest for the development of more robust transition metal catalysts and/or the utilization of more sustainable weaker bases.

Supporting Information

Complete experimental procedures, copies of NMR spectra for new compounds, full crystallographic data for compounds [**1f**](OTs) and **2b–f**, details of DFT calculations and Cartesian coordinates for all calculated structures. The authors have cited additional references within the Supporting Information.[51–67]

Acknowledgements

We thank joint CNRS/RFBR grant no. 19-53-15014 (PRC2330), Centre National de la Recherche Scientifique (CNRS), Université Toulouse III, Paul Sabatier (UPS) and Institut Universitaire de France (IUF) for general support of this work. E.S.G. is grateful to the French Embassy in Moscow for a joint PhD fellowship (Vernadski program). R.B. is indebted to the Embassy of Yemen in Paris and the program Pause for financial support. K.A. thanks the "Région Occitanie" for PhD fellowship. Computational studies were performed using HPC resources from CALMIP (grant no. P18038). Spectroscopic data were partially collected using the equipment of the Center for Molecular Composition Studies of INEOS RAS with the support from the Ministry of Science and Higher Education of the Russian Federation (contract no. 075-03-2023-642).

Conflict of Interests

The authors declare no conflict of interest.

Data Availability Statement

The data that support the findings of this study are available in the supplementary material of this article.

Keywords: Density functional calculations · Hydrogenation · Manganese · *N*-heterocyclic carbenes · Phosphorus ylides

[1] a) M. R. Elsby, R. T. Baker, *Chem. Soc. Rev.* **2020**, *49*, 8933–8987; b) J. R. Khusnutdinova, D. Milstein, *Angew. Chem. Int. Ed.* **2015**, *54*, 12236–12273.
[2] a) L. Alig, M. Fritz, S. Schneider, *Chem. Rev.* **2019**, *119*, 2681–2751; b) C. Gunanathan, D. Milstein, *Chem. Rev.* **2014**, *114*, 12024–12087.
[3] J. Zhang, G. Leitus, Y. Ben-David, D. Milstein, *J. Am. Chem. Soc.* **2005**, *127*, 10840–10841.
[4] PNN and NNN cooperative ligands: a) T. Cheisson, L. Mazaud, A. Auffrant, *Dalton Trans.* **2018**, *47*, 14521–14530; b) E. Fogler, J. A. Garg, P. Hu, G. Leitus, L. J. W. Shimon, D. Milstein, *Chem. Eur. J.* **2014**, *20*, 15727–15731.
[5] PNC and CNC cooperative ligands: a) P. Sánchez, M. Hernández-Juárez, N. Rendón, J. López-Serrano, E. Álvarez, M. Paneque, A. Suárez, *Organometallics* **2021**, *40*, 1314–1327; b) P. Sánchez, M. Hernández-Juárez, E. Álvarez, M. Paneque, N. Rendón, A. Suárez, *Dalton Trans.* **2016**, *45*, 16997–17009; c) G. A. Filonenko, E. Cosimi, L. Lefort, M. P. Conley, C. Copéret, M. Lutz, E. J. M. Hensen, E. A. Pidko, *ACS Catal.* **2014**, *4*, 2667–2671.
[6] PNS and SNS cooperative ligands: a) M. Gargir, Y. Ben-David, G. Leitus, Y. Diskin-Posner, L. J. W. Shimon, D. Milstein, *Organometallics* **2012**, *31*, 6207–6214; b) M. J. Page, J. Wagler, B. A. Messerle, *Organometallics* **2010**, *29*, 3790–3798.
[7] a) D. P. Zobernig, M. Luxner, B. Stöger, L. F. Veiros, K. Kirchner, *Chem. Eur. J.* **2023**, *30*, e202302455; b) S. Tang, N. von Wolff, Y. Diskin-Posner, G. Leitus, Y. Ben-David, D. Milstein, *J. Am. Chem. Soc.* **2019**, *141*, 7554–7561; c) A. J. Kosanovich, C. H. Komatsu, N. Bhuvanesh, L. M. Pérez, O. V. Ozerov, *Chem. Eur. J.* **2018**, *24*, 13754–13757; d) O. Rivada-Wheelaghan, A. Dauth, G. Leitus, Y. Diskin-Posner, D. Milstein, *Inorg. Chem.* **2015**, *54*, 4526–4538.
[8] a) A. B. Shabade, D. M. Sharma, P. Bajpai, R. G. Gonnade, K. Vanka, B. Punji, *Chem. Sci.* **2022**, *13*, 13764–13773; b) S. Michlik, R. Kempe, *Nat. Chem.* **2013**, *5*, 140–144; c) L. He, T. Chen, D. Gong, Z. Lai, K. Huang, *Organometallics* **2012**, *31*, 5208–5211; d) D. Benito-Garagorri, E. Becker, J. Wiedermann, W. Lackner, M. Pollak, K. Mereiter, J. Kisala, K. Kirchner, *Organometallics* **2006**, *25*, 1900–1913.
[9] W. H. Bernskoetter, S. K. Hanson, S. K. Buzak, Z. Davis, P. S. White, R. Swartz, K. I. Goldberg, M. Brookhart, *J. Am. Chem. Soc.* **2009**, *131*, 8603–8613.
[10] a) D. K. Pandey, E. Khaskin, J. R. Khusnutdinova, *ChemCatChem* **2023**, *15*, e202300644; b) D. K. Pandey, E. Khaskin, S. Pal, R. R. Fayzullin, J. R. Khusnutdinova, *ACS Catal.* **2023**, *13*, 375–381; c) B. Lee, T. P. Pabst, P. J. Chirik, *Organometallics* **2021**, *40*, 3766–3774; d) S. Lapointe, E. Khaskin, R. R. Fayzullin, J. R. Khusnutdinova, *Organometallics* **2019**, *38*, 4433–4447; e) S. Lapointe, E. Khaskin, R. R. Fayzullin, J. R. Khusnutdinova, *Organometallics* **2019**, *38*, 1581–1594.
[11] a) R. Stichauer, D. Duvinage, R. Langer, M. Vogt, *Organometallics* **2022**, *41*, 2798–2809; b) A. Mukherjee, A. Nerush, G. Leitus, L. J. W. Shimon, Y. Ben-David, N.-A. Espinosa-Jalapa, D. Milstein, *J. Am. Chem. Soc.* **2016**, *138*, 4298–4301; c) M. Montag, J. Zhang, D. Milstein, *J. Am. Chem. Soc.* **2012**, *134*, 10325–10328.
[12] C. A. Huff, J. W. Kampf, M. S. Sanford, *Chem. Commun.* **2013**, *49*, 7147–7149.
[13] a) K. Schlenker, E. G. Christensen, A. A. Zhanserkeev, G. R. McDonald, E. L. Yang, K. T. Lutz, R. P. Steele, R. T. VanderLinden, C. T. Saouma, *ACS Catal.* **2021**, *11*, 8358–8369; b) G. A. Filonenko, M. P. Conley, C. Copéret, M. Lutz, E. J. M. Hensen, E. A. Pidko, *ACS Catal.* **2013**, *3*, 2522–2526; c) C. A. Huff, M. S. Sanford, *ACS Catal.* **2013**, *3*, 2412–2416; d) M. Vogt, M. Gargir, M. A. Iron, Y. Diskin-Posner, Y. Ben-David, D. Milstein, *Chem. Eur. J.* **2012**, *18*, 9194–9197.
[14] J. Bruffaerts, N. von Wolff, Y. Diskin-Posner, Y. Ben-David, D. Milstein, *J. Am. Chem. Soc.* **2019**, *141*, 16486–16493.
[15] a) A. Nerush, M. Vogt, U. Gellrich, G. Leitus, Y. Ben-David, D. Milstein, *J. Am. Chem. Soc.* **2016**, *138*, 6985–6997; b) S. Perdriau, D. S. Zijlstra, H. J. Heeres, J. G. de Vries, E. Otten, *Angew. Chem. Int. Ed.* **2015**, *54*, 4236–4240; c) M. Vogt, A. Nerush, M. A. Iron, G. Leitus, Y. Diskin-Posner, L. J. W. Shimon, Y. Ben-David, D. Milstein, *J. Am. Chem. Soc.* **2013**, *135*, 17004–17018.
[16] For optically-active phosphine-pyridine ligands, see: a) R. Postolache, J. M. Pérez, M. Castiñeira Reis, L. Ge, E. G. Sinnema, S. R. Harutyunyan, *Org. Lett.* **2023**, *25*, 1611–1615; b) J. M. Pérez, R. Postolache, M. Castiñeira Reis, E. G. Sinnema, D. Vargová, F. de Vries, E. Otten, L. Ge, S. R. Harutyunyan, *J. Am. Chem. Soc.* **2021**, *143*, 20071–20076; c) Y. Huang, R. J. Chew, Y. Li, S. A. Pullarkat, P.-H. Leung, *Org. Lett.* **2011**, *13*, 5862–5865; d) F. Liu, S. A. Pullarkat, Y. Li, S. Chen, M. Yuan, Z. Y. Lee, P.-H. Leung, *Organometallics* **2009**, *28*, 3941–3946; e) H. Yang, M. Alvarez-Gressier, N. Lugan, R. Mathieu, *Organometallics* **1997**, *16*, 1401–1409; f) Q. Jiang, D. Van Plew, S. Murtuza, X. Zhang, *Tetrahedron Lett.* **1996**, *37*, 797–800.
[17] Complexes with bridge-substituted bidentate PN ligands: a) G. Si, Y. Na, C. Chen, *ChemCatChem* **2018**, *10*, 5135–5140; b) D. Schiefer, T. Wen, Y. Wang, P. Goursot, H. Komber, R. Hanselmann, P. Braunstein, G. Reiter, M. Sommer, *ACS Macro Lett.* **2014**, *3*, 617–621; c) F. Speiser, P. Braunstein, L. Saussine, *Organometallics* **2004**, *23*, 2625–2632; d) H. Brunner, A. Köllnberger, A. Mehmood, T. Tsuno, M. Zabel, *J. Organomet. Chem.* **2004**, *689*, 4244–4262; e) H. Yang, H. Gao, R. J. Angelici, *Organometallics* **2000**, *19*, 622–629; f) H. Yang, H. Gao, R. J. Angelici, *Organometallics* **1999**, *18*, 2285–2287.
[18] Complexes with bridge-substituted pincer-type PNP ligands: a) S. Deolka, N. Tarannam, R. R. Fayzullin, S. Kozuch, E. Khaskin, *Chem. Commun.* **2019**, *55*, 11350–11353; b) J. I. van der Vlugt, E. A. Pidko, D. Vogt, M. Lutz, A. L. Spek, *Inorg. Chem.* **2009**, *48*, 7513–7515.
[19] R. Buhaibeh, O. A. Filippov, A. Bruneau-Voisine, J. Willot, C. Duhayon, D. A. Valyaev, N. Lugan, Y. Canac, J.-B. Sortais, *Angew. Chem. Int. Ed.* **2019**, *58*, 6727–6731.
[20] N. V. Kireev, O. A. Filippov, E. S. Gulyaeva, E. S. Shubina, L. Vendier, Y. Canac, J.-B. Sortais, N. Lugan, D. A. Valyaev, *Chem. Commun.* **2020**, *56*, 2139–2142.
[21] A. M. King, H. A. Sparkes, R. L. Wingad, D. F. Wass, *Organometallics* **2020**, *39*, 3873–3878.
[22] D. A. Valyaev, O. A. Filippov, N. Lugan, G. Lavigne, N. A. Ustynyuk, *Angew. Chem. Int. Ed.* **2015**, *54*, 6315–6319.
[23] Deposition numbers 2313612 (for **2b**), 2313613 (for **2c**), 2313614 (for **2d**), 2313615 (for **2e**), 2313616 (for **2f**) and 2313617 (for [**1f**](OTs) contain the supplementary crystallographic data for this paper. These data are provided free of charge by the joint Cambridge Crystallographic Data Centre and Fachinformationszentrum Karlsruhe Access Structures service.
[24] a) K. Das, S. Waiba, A. Jana, B. Maji, *Chem. Soc. Rev.* **2022**, *51*, 4386–4464; b) E. S. Gulyaeva, E. S. Osipova, R. Buhaibeh, Y. Canac, J.-B. Sortais, D. A. Valyaev, *Coord. Chem. Rev.* **2022**, *458*, 214421; c) Y. Wang, M. Wang, Y. Li, Q. Liu, *Chem* **2021**, *7*, 1180–1223.
[25] Pincer-type Mn(I) complexes: a) N. F. Both, A. Spannenberg, H. Jiao, K. Junge, M. Beller, *Angew. Chem. Int. Ed.* **2023**, *62*, e202307987; b) Z. Wei, H. Li, Y. Wang, Q. Liu, *Angew. Chem. Int. Ed.* **2023**, *62*, e202301042; c) C. L. Oates, A. S. Goodfellow, M. Bühl, M. L. Clarke, *Angew. Chem. Int. Ed.* **2022**, *62*, e202212479; d) R. Buhaibeh, C. Duhayon, D. A. Valyaev, J.-B. Sortais, Y. Canac, *Organometallics* **2021**, *40*, 231–241; e) C. S. G. Seo, B. T. H. Tsui, M. V. Gradiski, S. A. M. Smith, R. H. Morris, *Catal. Sci. Technol.* **2021**, *11*, 3153–3163; f) L. Zhang, Z. Wang, Z. Han, K. Ding, *Angew. Chem. Int. Ed.* **2020**, *59*, 15565–15569; g) L. Zhang, Y. Tang, Z. Han, K. Ding, *Angew. Chem. Int. Ed.* **2019**, *58*, 4973–4977; h) F. Ling, H. Hou, J. Chen, S. Nian, X. Yi, Z. Wang, D. Song, W. Zhong, *Org. Lett.* **2019**, *21*, 3937–3941; i) M. B. Widegren, M. L. Clarke, *Catal. Sci. Technol.* **2019**, *9*, 6047–6058; j) A. Passera, A. Mezzetti, *Adv. Synth. Catal.* **2019**, *361*, 4691–4706; k) M. B. Widegren, G. J. Harkness, A. M. Z. Slawin, D. B. Cordes, M. L. Clarke, *Angew. Chem. Int. Ed.* **2017**, *56*, 5825–5828; l) M. Garbe, K. Junge, S. Walker, Z. Wei, H. Jiao, A. Spannenberg, S. Bachmann, M. Scalone, M. Beller, *Angew. Chem. Int. Ed.* **2017**, *56*, 11237–11241; m) F. Kallmeier, T. Irrgang, T. Dietel, R. Kempe, *Angew. Chem. Int. Ed.* **2016**, *55*, 11806–11809; n) S. Elangovan, C. Topf, S. Fischer, H. Jiao, A. Spannenberg, W. Baumann, R. Ludwig, K. Junge, M. Beller, *J. Am. Chem. Soc.* **2016**, *138*, 8809–8814.
[26] Mn(I) complexes bearing bidentate ligands: a) F. Wiedemaier, M. Rath, A. Reisenhofer, A. Dupé, F. Belaj, N. C. Mösch-Zanetti, *J. Catal.* **2023**, 115252; b) S. Weber, J. Brünig, L. F. Veiros, K. Kirchner, *Organometallics* **2021**, *40*, 1388–1394; c) H.-J. Pan, X. Hu, *Angew. Chem. Int. Ed.* **2020**, *59*, 4942–4946; d) S. Weber, B. Stöger, K. Kirchner, *Org. Lett.* **2018**, *20*, 7212–7215; e) D. Wei, A. Bruneau-Voisine, T. Chauvin, V. Dorcet, T. Roisnel, D. A. Valyaev, N. Lugan, J.-B. Sortais, *Adv. Synth. Catal.* **2018**, *360*, 676–681.
[27] W. Yang, I. Y. Chernyshov, R. K. A. van Schendel, M. Weber, C. Müller, G. A. Filonenko, E. A. Pidko, *Nat. Commun.* **2021**, *12*, 12.
[28] a) E. S. Gulyaeva, E. S. Osipova, S. A. Kovalenko, O. A. Filippov, N. V. Belkova, L. Vendier, Y. Canac, E. S. Shubina, D. A. Valyaev, *Chem. Sci.* **2024**, *15*, 1409–1417; b) R. Kumar, M. K. Pandey, A. Bhandari, J. Choudhury, *ACS Catal.* **2023**, *13*, 4824–4834; c) W. Yang, T. Y. Kalavalapalli, A. M. Krieger, T. A. Khvorost, I. Y. Chernyshov, M. Weber, E. A. Uslamin, E. A. Pidko, G. A. Filonenko, *J. Am. Chem. Soc.* **2022**, *144*, 8129–8137; d) K. Ganguli, A. Mandal, S. Kundu, *ACS Catal.* **2022**, *12*, 12444–12457.

[29] V. Vigneswaran, P. C. Abhyankar, S. N. MacMillan, D. C. Lacy, *Organometallics* **2021**, *41*, 67–75.
[30] E. S. Osipova, E. S. Gulyaeva, N. V. Kireev, S. A. Kovalenko, C. Bijani, Y. Canac, D. A. Valyaev, O. A. Filippov, N. V. Belkova, E. S. Shubina, *Chem. Commun.* **2022**, *58*, 5017–5020.
[31] K. Azouzi, L. Pedussaut, R. Pointis, A. Bonfiglio, R. Kumari Riddhi, C. Duhayon, S. Bastin, J.-B. Sortais, *Organometallics* **2023**, *42*, 1832–1838.
[32] K. B. Wiberg, *Tetrahedron* **1968**, *24*, 1083–1096.
[33] C. H. Leung, C. D. Incarvito, R. H. Crabtree, *Organometallics* **2006**, *25*, 6099–6107.
[34] G. Sipos, A. Ou, B. W. Skelton, L. Falivene, L. Cavallo, R. Dorta, *Chem. Eur. J.* **2016**, *22*, 6939–6946.
[35] D. Fenske, K. Brandt, P. Stock, *Z. Naturforsch.* **1981**, *36b*, 768–770.
[36] Y. Nakajima, F. Ozawa, *Organometallics* **2012**, *31*, 2009–2015.
[37] a) M. El Kadiri, A. Chihab, R. Taakili, C. Duhayon, D. A. Valyaev, Y. Canac, *Organometallics* **2022**, *41*, 456–466; b) R. Taakili, C. Barthes, C. Lepetit, C. Duhayon, D. A. Valyaev, Y. Canac, *Inorg. Chem.* **2021**, *60*, 12116–12128; c) R. Taakili, C. Barthes, A. Goëffon, C. Lepetit, C. Duhayon, D. A. Valyaev, Y. Canac, *Inorg. Chem.* **2020**, *59*, 7082–7096; d) R. Taakili, C. Lepetit, C. Duhayon, D. A. Valyaev, N. Lugan, Y. Canac, *Dalton Trans.* **2019**, *48*, 1709–1721; e) C. Barthes, C. Bijani, N. Lugan, Y. Canac, *Organometallics* **2018**, *37*, 673–678; f) I. Benaissa, R. Taakili, N. Lugan, Y. Canac, *Dalton Trans.* **2017**, *46*, 12293–12305; g) Y. Canac, C. Lepetit, M. Abdalilah, C. Duhayon, R. Chauvin, *J. Am. Chem. Soc.* **2008**, *130*, 8406–8413.
[38] A. W. Johnson Ed., *Ylides and Imines of Phosphorus*, John Wiley & Sons, New York **1993**.
[39] A. Das, S. C. Mandal, B. Pathak, *Catal. Sci. Technol.* **2021**, *11*, 1375–1385.
[40] P. A. Dub, J. C. Gordon, *ACS Catal.* **2017**, *7*, 6635–6655.
[41] E. S. Osipova, S. A. Kovalenko, E. S. Gulyaeva, N. V. Kireev, A. A. Pavlov, O. A. Filippov, A. A. Danshina, D. A. Valyaev, Y. Canac, E. S. Shubina, N. V. Belkova, *Molecules* **2023**, *28*, 3368.
[42] a) Y. Wang, S. Liu, H. Yang, H. Li, Y. Lan, Q. Liu, *Nat. Chem.* **2022**, *14*, 1233–1241; b) A. S. Tossaint, C. Rebreyend, V. Sinha, M. Weber, S. Canossa, E. A. Pidko, G. A. Filonenko, *Catal. Sci. Technol.* **2022**, *12*, 2972–2977; c) F. Freitag, T. Irrgang, R. Kempe, *J. Am. Chem. Soc.* **2019**, *141*, 11677–11685; d) C. L. Mathis, J. Geary, Y. Ardon, M. S. Reese, M. A. Philliber, R. T. VanderLinden, C. T. Saouma, *J. Am. Chem. Soc.* **2019**, *141*, 14317–14328.
[43] E. Fogler, J. A. Garg, P. Hu, G. Leitus, L. J. W. Shimon, D. Milstein, *Chem. Eur. J.* **2014**, *20*, 15727–15731.
[44] The implication of anionic hydride intermediates may be proposed in the asymmetric hydrogenation of *3H*-indoles and quinoxalines catalyzed by Mn(I) PNN complexes incorporating *1H*-imidazole extremity due to the observed strong influence of alkali-metal cation on the reaction output and highly detrimental effect of the *N*-methylation of the imidazole moiety, see: a) C. Liu, X. Liu, Q. Liu, *Chem* **2023**, *9*, 2585–2600; b) C. Liu, M. Wang, Y. Xu, Y. Li, Q. Liu, *Angew. Chem. Int. Ed.* **2022**, *61*, e202202814.
[45] F. Wiedemaier, F. Belaj, N. C. Mösch-Zanetti, *J. Catal.* **2022**, *416*, 103–111.
[46] M. Ameskal, R. Taakili, E. S. Gulyaeva, C. Duhayon, J. Willot, N. Lugan, C. Lepetit, D. A. Valyaev, Y. Canac, *Inorg. Chem.* **2023**, *62*, 20129–20141.
[47] a) K. Schlenker, L. K. Casselman, R. T. VanderLinden, C. T. Saouma, *Catal. Sci. Technol.* **2023**, *13*, 1358–1368; b) T.-Y. Cheng, B. S. Brunschwig, R. M. Bullock, *J. Am. Chem. Soc.* **1998**, *120*, 13121–13137.
[48] I. E. Golub, O. A. Filippov, N. V. Belkova, L. M. Epstein, E. S. Shubina, *J. Organomet. Chem.* **2018**, *865*, 247–256.
[49] For calculated external hydride transfer processes to ketones, imines and CO_2 implicating neutral Mn(I) complexes bearing bidentate ligands, see: a) Y. Jing, J. Liu, Z. Ye, J. Su, Y. Liu, Z. Ke, *Catal. Sci. Technol.* **2021**, *11*, 7189–7199; b) Y. Jing, Z. Ye, J. Su, Y. Feng, L.-B. Qu, Y. Liu, Z. Ke, *Catal. Sci. Technol.* **2020**, *10*, 5443–5447; c) M. Huang, Y. Li, Y. Li, J. Liu, S. Shu, Y. Liu, Z. Ke, *Chem. Commun.* **2019**, *55*, 6213–6216; d) X.-B. Lan, Z. Ye, M. Huang, J. Liu, Y. Liu, Z. Ke, *Org. Lett.* **2019**, *21*, 8065–8070.
[50] Despite slightly lower activation barrier located for external hydride transfer from meridional isomer of *mer*-(*C̈*)-[**7**]$^-$ to acetophenone, the implication of such species in this case seems to be unlikely due to its much lower thermodynamic stability *vs.* major facial isomer (see the Supporting Information).
[51] A. J. Arduengo III, F. P. Gentry Jr., P. K. Taverkere, H. E. Howard III, US Patent, **2001**, 6177 575.
[52] T. Chatterjee, N. T. Kumar, S. K. Das, *Polyhedron* **2017**, *127*, 68–83.
[53] M. Mihorianu, M. H. Franz, P. G. Jones, M. Freytag, G. Kelter, H.-H. Fiebig, M. Tamm, I. Neda, *Appl. Organomet. Chem.* **2016**, ***30***, 581–589.
[54] A. Plikhta, A. Pöthig, E. Herdtweck, B. Rieger, *Inorg. Chem.* **2015**, *54*, 9517–9528.
[55] P. A. Rudd, S. Liu, L. Gagliardi, V. G. Young Jr., C. C. Lu, *J. Am. Chem. Soc.* **2011**, *133*, 20724–20727.
[56] H. J. Clark, R. Wang, H. Alper, *J. Org. Chem.* **2002**, *67*, 6224–6225.
[57] L. Palatinus, G. Chapuis, *J. Appl. Crystallogr.* **2007**, *40*, 786–790.
[58] M. C. Burla, R. Caliandro, B. Carrozzini, G. L. Cascarano, C. Cuocci, C. Giacovazzo, M. Mallamo, A. Mazzone, G. Polidori, *J. Appl. Crystallogr.* **2015**, *48*, 306–309.
[59] P. W. Betteridge, J. R. Carruthers, R. I. Cooper, K. Prout, D. J. Watkin, *J. Appl. Crystallogr.* **2003**, *36*, 1487.
[60] G. M. Sheldrick, *Acta Crystallogr.* **2015**, *A71*, 3–8.
[61] R. H. Blessing, *Acta Crystallogr.* **1995**, *A51*, 33–38.
[62] M. J. Frisch, G. W. Trucks, H. B. Schlegel, G. E. Scuseria, M. A. Rob, J. R. Cheeseman, J. A. Montgomery Jr., T. Vreven, K. N. Kudin, J. C. Burant, J. M. Millam, S. S. Iyengar, J. Tomasi, V. Barone, B. Mennucci, M. Cossi, G. Scalmani, N. Rega, G. A. Petersson, H. Nakatsuji, M. Hada, M. Ehara, K. Toyota, R. Fukuda, J. Hasegawa, M. Ishida, T. Nakajima, Y. Honda, O. Kitao, H. Nakai, M. Klene, X. Li, J. E. Knox, H. P. Hratchian, J. B. Cross, V. Bakken, C. Adamo, J. Jaramillo, R. Gomperts, R. E. Stratmann, O. Yazyev, A. J. Austin, R. Cammi, C. Pomelli, J. W. Ochterski, P. Y. Ayala, K. Morokuma, G. A. Voth, P. Salvador, J. J. Dannenberg, V. G. Zakrzewski, S. Dapprich, A. D. Daniels, M. C. Strain, O. Farkas, D. K. Malick, A. D. Rabuck, K. Raghavachari, J. B. Foresman, J. V. Ortiz, Q. Cui, A. G. Baboul, S. Clifford, J. Cioslowski, B. B. Stefanov, G. Liu, A. Liashenko, P. Piskorz, I. Komaromi, R. L. Martin, D. J. Fox, T. Keith, M. A. Al-Laham, C. Y. Peng, A. Nanayakkara, M. Challacombe, P. M. W. Gill, B. Johnson, W. Chen, M. W. Wong, C. Gonzalez, J. A. Pople, *Gaussian, Inc.*, Wallingford, CT **2009**.
[63] a) A. D. Becke, *Phys. Rev. A* **1988**, *38*, 3098–3100; b) J. P. Perdew, *Phys. Rev. B* **1986**, *33*, 8822–8824.
[64] J.-D. Chai, M. Head-Gordon, *Phys. Chem. Chem. Phys.* **2008**, *10*, 6615–6620.
[65] a) F. Weigend, *Phys. Chem. Chem. Phys.* **2006**, *8*, 1057–1065; b) F. Weigend, R. Ahlrichs, *Phys. Chem. Chem. Phys.* **2005**, *7*, 3297–3305.
[66] A. V. C. C. J. Marenich, D. G. Truhlar, C. J. Cramer, *J. Phys. Chem. B* **2009**, *113*, 6378–6396.
[67] a) K. Fukui, *Acc. Chem. Res.* **1981**, *14*, 363–406; b) H. P. Hratchian, H. B. Schlegel, *Theory and Applications of Computational Chemistry*, G. Frenking, K. S. Kim, G. E. Scuseria Eds., Elsevier, Amsterdam **2005**.

Manuscript received: December 17, 2023
Accepted manuscript online: February 5, 2024
Version of record online: ■■, ■■

RESEARCH ARTICLE

Bridge substituent matters: the incorporation of phenyl group into the methylene bridge of bidentate phosphine-*N*-heterocyclic carbene (NHC) ligand leads to significant increase of catalytic performance for the corresponding Mn(I) complex. Mechanistic studies revealed that this effect was caused by stabilization of key metal intermediates including a highly reactive anionic hydride complex due to more efficient negative charge delocalization.

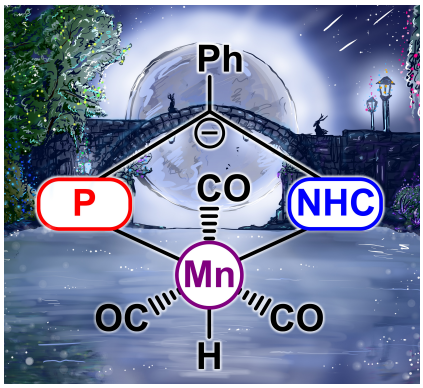

E. S. Gulyaeva, Dr. R. Buhaibeh, M. Boundor, Dr. K. Azouzi, Dr. J. Willot, Dr. S. Bastin, Dr. C. Duhayon, Dr. N. Lugan, Dr. O. A. Filippov, Prof. Dr. J.-B. Sortais, Dr. D. A. Valyaev*, Dr. Y. Canac**